PakB binds to the SH3 domain of *Dictyostelium* Abp1 and regulates its effects on cell polarity and early development

Yidai Yang, Marc de la Roche, Scott W. Crawley, Zhihao Li, Emilia Furmaniak-Kazmierczak, and Graham P. Côté
Department of Biomedical and Molecular Sciences, Queen's University, Kingston, ON K7L 3N6, Canada

ABSTRACT ***Dictyostelium*** **p21-activated kinase B (PakB) phosphorylates and activates class I myosins. PakB colocalizes with myosin I to actin-rich regions of the cell, including macropinocytic and phagocytic cups and the leading edge of migrating cells. Here we show that residues 1–180 mediate the cellular localization of PakB. Yeast two-hybrid and pull-down experiments identify two proline-rich motifs in PakB-1-180 that directly interact with the SH3 domain of *Dictyostelium* actin-binding protein 1 (dAbp1). dAbp1 colocalizes with PakB to actin-rich regions in the cell. The loss of dAbp1 does not affect the cellular distribution of PakB, whereas the loss of PakB causes dAbp1 to adopt a diffuse cytosolic distribution. Cosedimentation studies show that the N-terminal region of PakB (residues 1–70) binds directly to actin filaments, whereas dAbp1 exhibits only a low affinity for filamentous actin. PakB-1-180 significantly enhances the binding of dAbp1 to actin filaments. When overexpressed in PakB-null cells, dAbp1 completely blocks early development at the aggregation stage, prevents cell polarization, and significantly reduces chemotaxis rates. The inhibitory effects are abrogated by the introduction of a function-blocking mutation into the dAbp1 SH3 domain. We conclude that PakB plays a critical role in regulating the cellular functions of dAbp1, which are mediated largely by its SH3 domain.**

Monitoring Editor
Carole Parent
National Institutes of Health

Received: Dec 14, 2012
Revised: May 13, 2013
Accepted: May 15, 2013

INTRODUCTION

The class I myosins are monomeric, single-headed molecules that function at the interface between cell membranes and the actin cytoskeleton (McConnell and Tyska, 2010). Class I myosins consist of a conserved motor domain that interacts with actin filaments to generate force, a neck region that binds light chains, and a tail that contains a tail homology 1 (TH1) domain that binds acidic phospholipids. The tails of some class I myosins are longer and have, in addition to the TH1 domain, a TH2 domain, which binds actin filaments, and a Src homology 3 (SH3) domain. The highly motile social amoeba *Dictyostelium discoideum* expresses seven class I myosins: MyoA, MyoE, and MyoF have short tails; MyoB, MyoC, and MyoD have long tails; and the atypical MyoK lacks a tail but contains a TH2-like insert in the motor domain. The *Dictyostelium* myosin I isozymes are implicated in a wide range of cellular functions, including endocytosis, macropinocytosis, phagocytosis, cortical tension generation, actin filament assembly, and formation and retraction of membrane projections (Novak *et al.*, 1995; Jung *et al.*, 1996, 2001; Dai *et al.*, 1999; Schwarz *et al.*, 2000; Falk *et al.*, 2003; Durrwang *et al.*, 2006; Chen *et al.*, 2012).

The motor activities of the *Dictyostelium* class I myosins depend on the phosphorylation of a serine or threonine residue at a position in the motor domain termed the TEDS site (Bement and Mooseker, 1995; Novak and Titus, 1998; Fujita-Becker *et al.*, 2004; Durrwang *et al.*, 2006). p21-activated kinase B (PakB), a member of the p21-activated kinase (PAK) family of serine/threonine protein kinases, can phosphorylate the TEDS site of MyoD, MyoK, and, to a lesser extent, MyoB (Lee and Côté, 1995; Lee *et al.*, 1996; Dieckmann *et al.*, 2010). PakB contains a proline-rich N-terminal region, a

This article was published online ahead of print in MBoC in Press (http://www.molbiolcell.org/cgi/doi/10.1091/mbc.E12-12-0883) on May 22, 2013.

Address correspondence to: Graham Côté (coteg@queensu.ca).

Abbreviations used: ADF-H, actin-depolymerizing factor homology; dAbp1, *Dictyostelium* actin-binding protein 1; GFP, green fluorescent protein; GST, glutathione *S*-transferase; PakB, p21-activated kinase B; PBD, p21-binding domain; RFP, red fluorescent protein; SH3, src homology 3.

conserved p21-binding domain (PBD) that recognizes the active GTP-bound forms of several *Dictyostelium* Racs, and a C-terminal kinase domain (Lee *et al.*, 1996; De La Roche *et al.*, 2005). The conversion of PakB from an inactive to an active state occurs in two distinct steps (Lee *et al.*, 1998). In the absence of allosteric effectors PakB autophosphorylates a single site, Ser-8, which increases kinase activity and allows the PBD to interact with activated Rac. Binding of activated Rac then promotes the autophosphorylation of multiple additional sites and produces a further 10-fold increase in PakB activity. PakB is also activated by acidic lipids in a reaction that is inhibited by Ca^{2+}-calmodulin (Lee *et al.*, 1998).

In growth-phase *Dictyostelium* cells PakB colocalizes with myosin I to dynamic actin-rich regions at the cell cortex, including macropinocytic and phagocytic cups and the tips of protruding pseudopods (De La Roche *et al.*, 2005; Dieckmann *et al.*, 2010). In starved *Dictyostelium* cells that elongate and chemotax in response to an extracellular cAMP gradient, PakB is enriched with myosin I at the actin-rich leading edge (De La Roche *et al.*, 2005). PakB-null ($PakB^-$) cells, like myosin I–null cells, lose polarity and extend multiple pseudopods during chemotaxis (Lee *et al.*, 2004). However, the defects exhibited by $PakB^-$ cells are quite mild, suggesting that its loss is compensated for by other protein kinases (Lee *et al.*, 2004; De La Roche *et al.*, 2005). There is evidence that PakC, which has an N-terminal region that contains a pleckstrin homology domain but shares very similar PBD and kinase domains with PakB, has overlapping functions with PakB in the regulation of polarity and chemotaxis (Lee *et al.*, 2004).

PakB is targeted to dynamic actin-rich regions of the cell cortex by its proline-rich N-terminal region (De La Roche *et al.*, 2005). In this article, we show that a short section of the N-terminal region of PakB mimics the cellular localization of the full-length protein. We demonstrate that this N-terminal segment contains an actin filament–binding module and two closely spaced proline-rich motifs that serve as docking sites for the SH3 domain of *Dictyostelium* actin-binding protein 1 (dAbp1). dAbp1 binds class I myosins and plays an important role in regulating cell polarity and pseudopod formation during chemotaxis (Wang and O'Halloran, 2006; Dieckmann *et al.*, 2010). dAbp1 is not needed for PakB to localize to dynamic actin-rich regions in the cell; instead, PakB recruits dAbp1 to these sites and is required to control or restrict the activities of dAbp1. The results support a model in which the PakB–dAbp1 complex plays a role in the regulation of class I myosins but show also that the interaction with PakB prevents dAbp1 from severely disrupting cellular processes needed for polarization, chemotaxis, and early development.

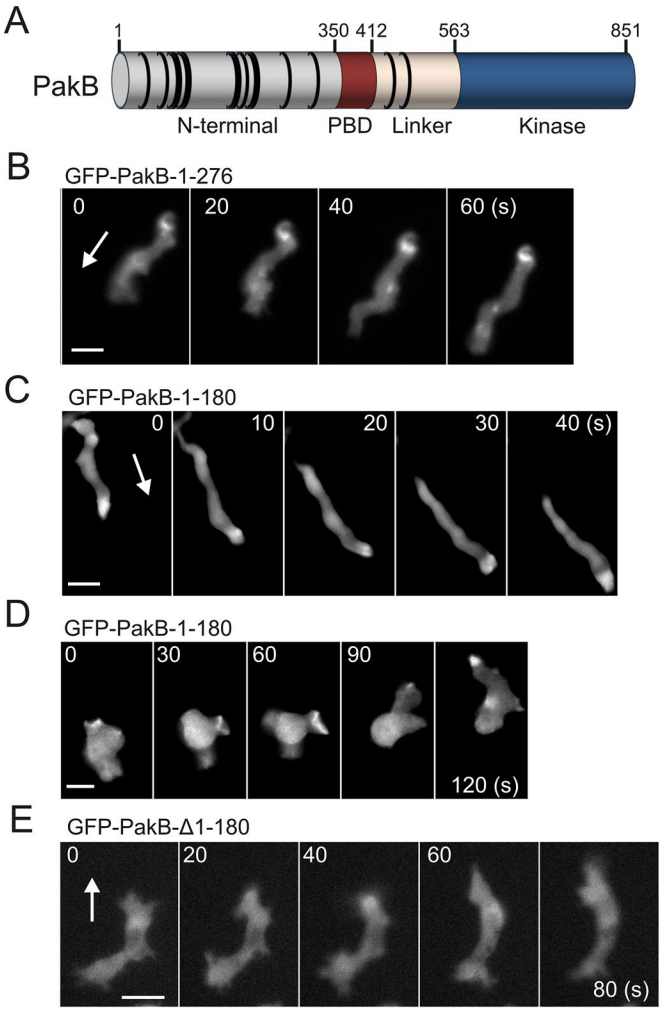

FIGURE 1: PakB-1-180 mimics the subcellular localization of PakB. (A) *Dictyostelium* PakB consists of a proline-rich, N-terminal domain, a p21-binding domain (PBD) that recognizes Rac GTPases, an unstructured linker segment, and a C-terminal Ser/Thr protein kinase domain. The positions of PxxP motifs are indicated by black rings. (B) Time-course images of GFP-PakB-1-276 expressed in an aggregation-competent AX3 cell migrating in a cAMP gradient. (C, D) Time-course images of GFP-PakB-1-180 expressed in (C) an aggregation-competent AX3 cell migrating in a cAMP gradient and (D) a growth-phase AX3 cell extending pseudopods and macropinocytic cups. (E) Time-course images of GFP-PakB lacking residues 1–180 (GFP-PakB-Δ1-180) expressed in an AX3 cell. Arrows indicate the direction of migration. Bars, 10 μm.

RESULTS

Residues 1–180 target PakB to the cell cortex

PakB consists of a proline-rich N-terminal region, a PBD domain, an unstructured linker region, and a C-terminal kinase domain (Figure 1A). Previous work showed that the N-terminal region is responsible for targeting PakB to dynamic actin-rich regions of the cell cortex, including macropinocytic and phagocytic cups, pseudopods, and the leading edge of migrating cells (Supplemental Figure S1, A and B; De La Roche *et al.*, 2005). To further define the sites responsible for the cellular localization of PakB, we expressed PakB residues 1–276 and 1–180 in cells as green fluorescent protein (GFP) fusion proteins. PakB-1-276 formed a small number of dot-like structures, which accumulated at the rear of migrating cells (Figure 1B and Supplemental Video S1). This behavior is reminiscent of PakB constructs that lack the PBD and linker regions (PakB-ΔPL) or the kinase domain (PakB-ΔC) and may be due to aggregation (De La Roche *et al.*, 2005). In contrast, the cellular localization of PakB-1-180 mimicked that of PakB. PakB-1-180 was enriched at the leading edge of migrating cells and transiently accumulated within macropinocytic cups (Figure 1, C and D, Supplemental Figures S1C and S2, and Supplemental Videos S2 and S3). Truncation of residues 1–180 prevented PakB from localizing to actin-rich regions of the cell (Figure 1D). The results show that residues 1–180 harbor the major determinants responsible for targeting PakB to the cell cortex.

PakB-1-180 binds the SH3 domain of dAbp1

To identify proteins that bind to PakB-1-180, we used it as the bait in a yeast two-hybrid screen of a *Dictyostelium* growth-phase cDNA library. A screen of 10^6 independent clones identified six interacting clones, all of which were verified by reintroduction of the rescued

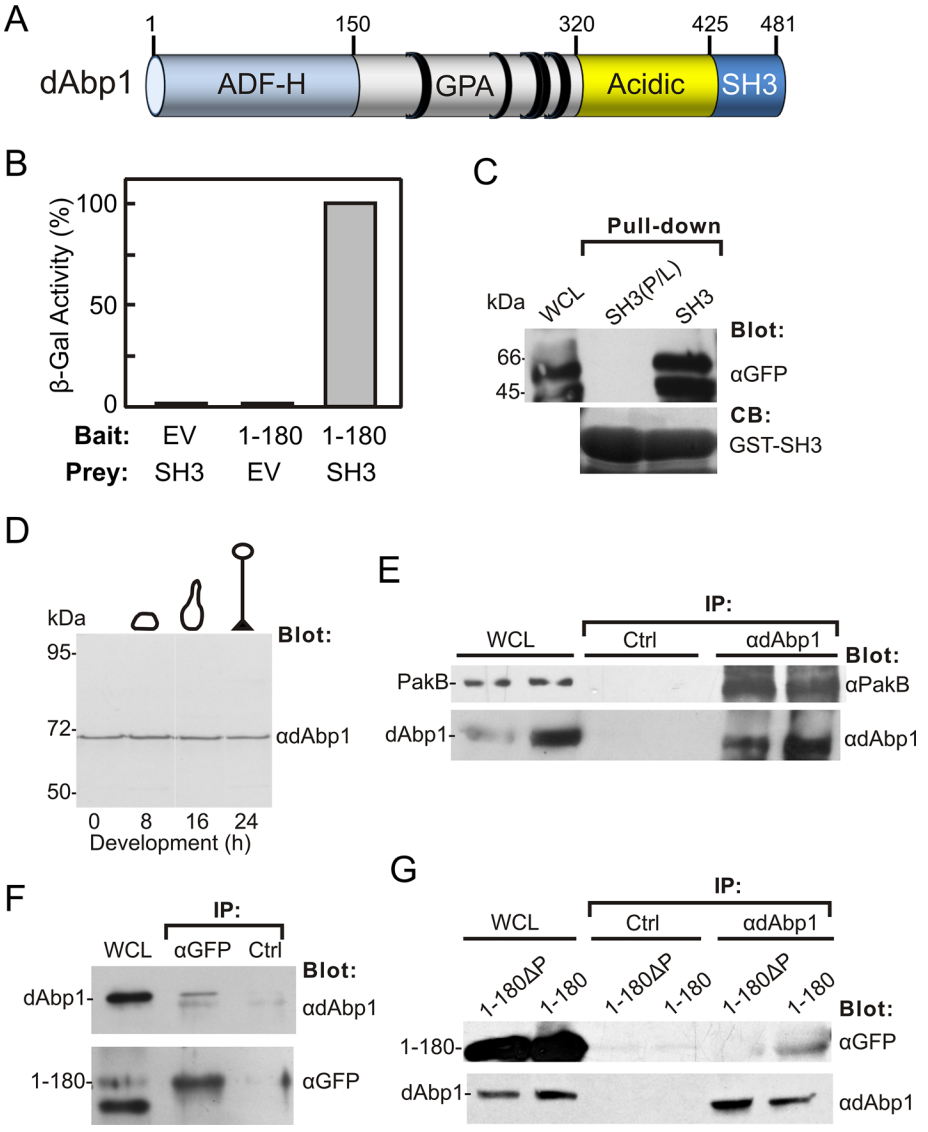

FIGURE 2: PakB-1-180 binds the dAbp1 SH3 domain. (A) dAbp1 consists of an ADF-H domain, a segment rich in glutamine, proline, and alanine (GPA) residues, a highly acidic region, and an SH3 domain. The positions of PxxP motifs are indicated by black rings. (B) Two-hybrid analysis was carried out using a bait vector expressing PakB-1-180 (1–180) and a prey vector expressing the dAbp1 SH3 domain (SH3) and empty bait or prey vectors (EV). The strength of the interaction was assessed quantitatively by liquid culture β-galactosidase assay. (C) Pull-down assays were carried out using the GST-dAbp1-SH3 domain (SH3) or an inactive GST-dAbp1-SH3 domain (P474L mutation; SH3(P/L)) and lysates of cells expressing GFP-PakB-1-180. The whole-cell lysate (WCL) and washed pellets were probed using an anti-GFP antibody. Coomassie blue (CB) was used to visualize the GST-SH3 domains in the pellets. (D) Immunoblot analysis of AX3 cells harvested at different stages of development using an affinity-purified rabbit polyclonal antibody to dAbp1. (E) Coimmunoprecipitation of endogenous dAbp1 and PakB. Immunoprecipitates were prepared from AX3 cell lysates using a control (Ctrl) or anti-dAbp1 antibody. The WCL and washed immunoprecipitates were immunoblotted using anti-PakB and anti-dAbp1 antibodies. Results from two experiments are shown. (F) Immunoprecipitates were prepared from lysates of cells expressing GFP-PakB-1-180 (1–180) using an anti-GFP antibody or a control (Ctrl) antibody. The WCL and washed immunoprecipitates were immunoblotted using antibodies to GFP and dAbp1. (G) Immunoprecipitates were prepared from cells expressing GFP-PakB-1-180 (1–180) or GFP-PakB-1-180ΔP (1-180ΔP) using an anti-dAbp1 or a control (Ctrl) antibody. The WCLs and washed immunoprecipitates were immunoblotted using antibodies to GFP and dAbp1.

plasmids back into the W303 yeast strain originally used in the screen. Three of the interacting clones encoded ribosomal proteins and three encoded fragments of dAbp1, the product of the *abpE* gene (dictyBase DDB_G0273447). dAbp1 consists of an N-terminal, actin-depolymerizing factor homology (ADF-H) domain, a basic region (pI 9.76) rich in glycine, proline, and alanine residues, a highly acidic region (pI 3.14), and a C-terminal SH3 domain (Figure 2A).

The interacting dAbp1 clones identified in the yeast two-hybrid assays were missing 100–200 base pairs at the 5′ end, demonstrating that an intact ADF-H domain is not required to bind PakB-1-180. Two-hybrid assays showed that the C-terminal SH3 domain of dAbp1 was responsible for the interaction with PakB-1-180 (Figure 2B). This interaction was confirmed by carrying out pull-down assays using a glutathione *S*-transferase (GST)–dAbp1-SH3 domain fusion protein and lysates of *Dictyostelium* cells expressing GFP-PakB-1-180 (Figure 2C). As a control, pull-down assays were also performed using a dAbp1 SH3 domain containing a predicted function-blocking point mutation (Pro-474 to leucine; Jung *et al.*, 2001). This mutation abolished the interaction between the GST-dAbp1-SH3 domain and PakB-1-180 (Figure 2C)

To carry out immunoprecipitation experiments, we raised a rabbit polyclonal antibody against GST-dAbp1. Immunoblot analysis showed that the antibody detected a single band of ~66 kDa when used to probe *Dictyostelium* cell extracts (Figure 2D). dAbp1 has a calculated molecular weight of 55.3 kDa, but the highly acidic region may cause it to electrophorese with a somewhat lower mobility. The level of expression of dAbp1 was relatively constant throughout *Dictyostelium* development. Coimmunoprecipitation experiments carried out using the anti-dAbp1 antibody showed an interaction between endogenous dAbp1 and PakB (Figure 2E). GFP-PakB-1-180 and dAbp1 were also found to interact when immunoprecipitates were prepared using either the anti-dAbp1 antibody or an anti-GFP antibody (Figure 2, F and G). On the basis of these results, we conclude that dAbp1 binds via its SH3 domain to residues 1–180 of PakB.

Mapping of the dAbp1-binding sites on PakB

The 1–180 sequence of PakB contains seven PxxP motifs (P1–P7), which could function as binding sites for the dAbp1 SH3 domain (Figure 3A). A PakB-1-120 fragment, which contains all seven PxxP motifs, bound to the SH3 domain of dAbp1 (Figure 3B). No interaction was detected between PakB-1-120 and the SH3 domains of the *Dictyostelium* class I myosins MyoB and MyoC (Figure 3B). The results suggest that the

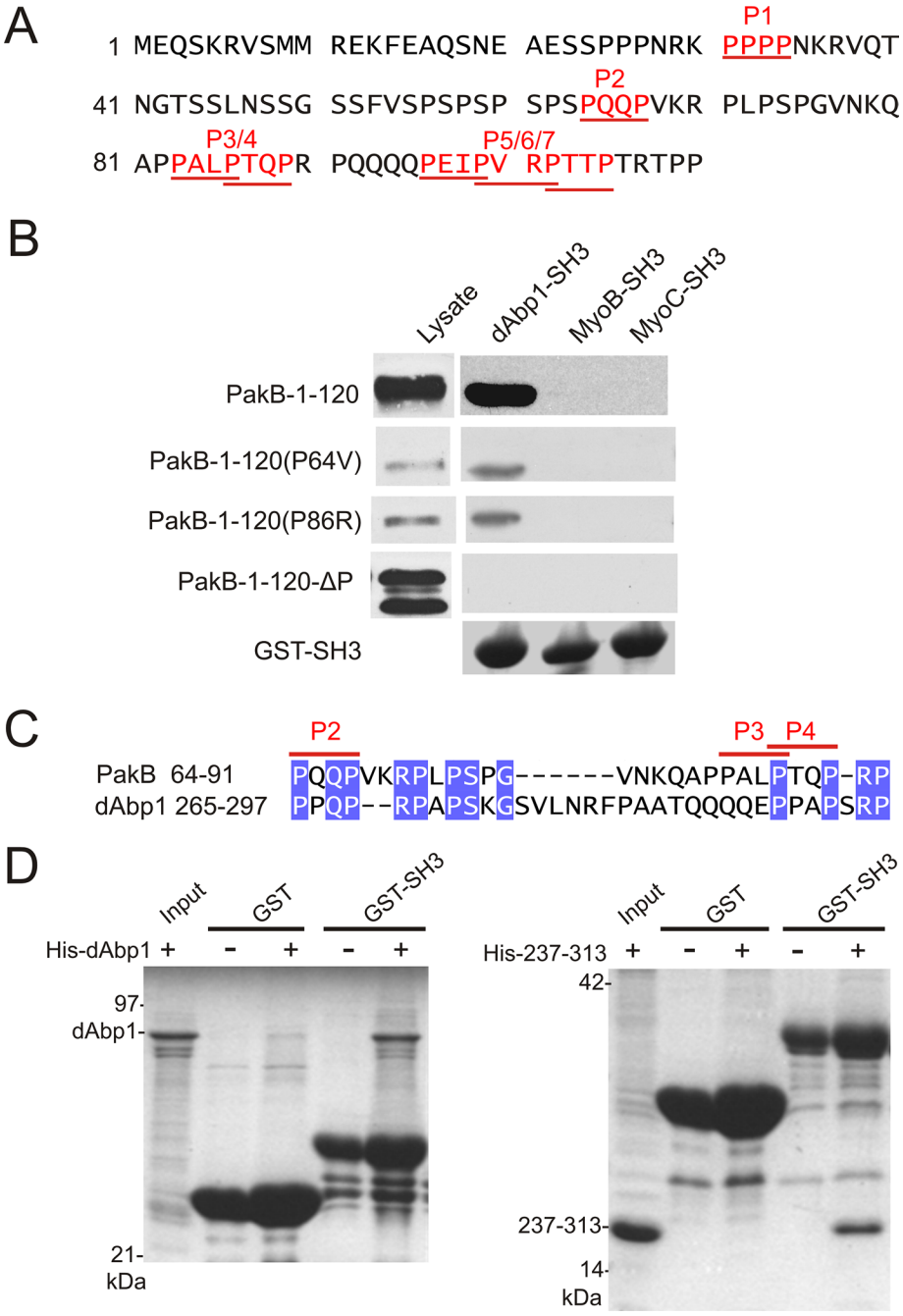

FIGURE 3: Identification of two binding sites for the dAbp1 SH3 domain in PakB. (A) The N-terminal region of PakB contains seven PxxP motifs (P1–P7; red underlined). (B) Pull-down assays were performed using GST fusion proteins containing the SH3 domains of dAbp1, MyoB, or MyoC and lysates of PakB$^-$ cells expressing the indicated GFP-PakB constructs. PakB-1-120 containing both the P64V and P86 mutations is designated PakB-1-120-ΔP. The cell lysates and washed pellets were subjected to immunoblot analysis using an anti-GFP antibody. GST-SH3 domains were visualized by Coomassie blue staining. (C) dAbp1 contains a proline-rich sequence similar to the P2–P3/4 region of PakB. (D) Pull-down assays were performed using GST (GST) or GST-dAbp1-SH3 (GST-SH3) and His-tagged dAbp1(His-dAbp1; left) or residues 237–313 of dAbp1 (His-237-313; right). The washed pellets were visualized by Coomassie blue staining after SDS–PAGE.

N-terminal region of PakB does not directly recruit class I myosins for phosphorylation by the kinase domain and also demonstrate the specificity of the interaction between PakB-1-120 and the dAbp1 SH3 domain.

Pull-down assays showed that mutations resulting in disruption of the P1, P2, P3/4, or P5/6/7 PxxP motifs did not block the binding interaction between PakB-1-120 and the dAbp1 SH3 domain. When combinations of mutations were tested, it was found that disruption of the P2 motif (P64V) together with the overlapping P3/P4 motifs (P86R) was required to abolish binding (Figure 3B). A PakB-1-180 mutant containing the P64V and P86R substitutions (PakB-1-180ΔP) was expressed in *Dictyostelium* as a GFP fusion protein. PakB-1-180ΔP did not coimmunoprecipitate with dAbp1, confirming that interaction between the two proteins involves direct binding of the dAbp1 SH3 domain to the P2 and P3/4 motifs of PakB (Figure 2G).

Of interest, dAbp1 contains a proline-rich sequence (residues 265–297) that shares a high degree of identity with the P2-P3/4 region of PakB (Figure 3C). This suggested that dAbp1 might contain an internal binding site for its SH3 domain. Pull-down assays were therefore carried out using GST-dAbp1-SH3 and either histidine (His)-tagged full-length dAbp1 or a His-tagged dAbp1-237-313 fragment. Both full-length dAbp1 and the fragment containing the P2-P3/4-like sequence bound to the GST-dAbp1-SH3 domain but not to GST alone (Figure 3D). The results suggest that dAbp1 could form dimers via an SH3 domain–mediated interaction or, alternatively, adopt a folded conformation in which the SH3 domain binds intramolecularly to the P2-P3/4–like region.

Localization of dAbp1 depends on PakB

Both dAbp1 and PakB are present in phagocytic cups and at the leading edge of migrating cells (De La Roche *et al.*, 2005; Wang and O'Halloran, 2006; Dieckmann *et al.*, 2010). Immunofluorescence analysis showed that PakB-1-180 and dAbp1 colocalized to macropinocytic cups and the leading edges of pseudopods (Figure 4A). To test whether PakB-1-180 is recruited to these actin-rich sites by dAbp1, we expressed PakB-1-180ΔP in cells. Surprisingly, the loss of the dAbp1-binding sites did not prevent recruitment of PakB-1-180ΔP to the leading edge of developed migrating cells to macropinocytic cups in growth-phase cells (Figure 4B, top). Similarly, GFP-PakB-1-180 localized to the leading edge and macropinocytic cups in dAbp1-null cells (Figure 4B, bottom; Dieckmann *et al.*, 2010). The results show that PakB-1-180 does not require dAbp1 to be targeted to actin-rich sites at the cell cortex.

We next examined the possibility that PakB is required to localize dAbp1. In agreement with previous results, red fluorescent protein

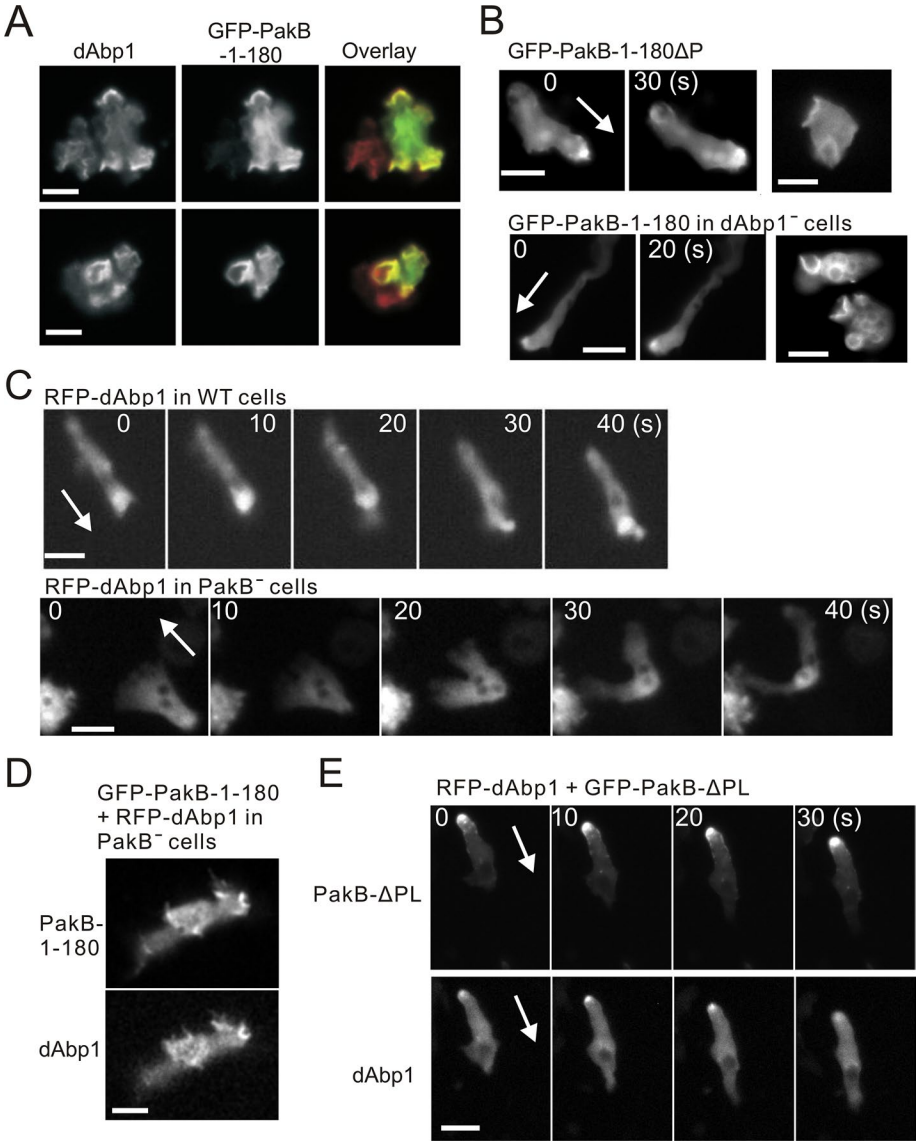

FIGURE 4: Colocalization of PakB and dAbp1. (A) AX3 cells expressing GFP-PakB-1-180 were fixed and stained using antibodies against dAbp1 and GFP. The overlay shows staining for GFP in green and dAbp1 in red. (B) Images of GFP-PakB-1-180ΔP expressed in PakB⁻ cells (top) and GFP-PakB-1-180 expressed in dAbp1-null (dAbp1⁻) cells (bottom). Migrating developed cells are shown in the left and middle, and growth-phase cells with macropinocytic cups are shown in the right. (C) RFP-dAbp1 was imaged in a developed migrating AX3 cell (top) and PakB⁻ cell (bottom). (D) Expression of GFP-PakB-1-180 in a PakB⁻ cell restores the cortical localization of RFP-dAbp1. (E) Expression of constitutively active GFP-PakB-ΔPL, which mislocalizes to the rear of migrating cells, results in recruitment of RFP-dAbp1 to the cell posterior. Arrows indicate the direction of migration. Bars, 10 μm.

(RFP)–dAbp1 was enriched at the leading edge of developed migrating wild-type cells (Figure 4C, top; Supplemental Video S4; Wang and O'Halloran, 2006). In migrating PakB⁻ cells, however, RFP-dAbp1 was diffusely distributed in the cytosol (Figure 4C, bottom; see also Figure 6C and Supplemental Video S5). The mislocalization of dAbp1 is not due to the absence of filamentous actin, since the actin-binding domain of ABP-120 (ABD), which serves as a marker for actin filaments, localized to the cortex and pseudopods of PakB⁻ cells (Supplemental Figure S3; Pang *et al.*, 1998). Moreover, the expression of PakB-1-180 restored the ability of dAbp1 to localize to the cortex of PakB⁻ cells (Figure 4D). The role of PakB in mediating the cellular localization of dAbp1 was further tested by expressing the constitutively active PakB-ΔPL, which mislocalizes to the rear of migrating cells (De La Roche *et al.*, 2005). When expressed in PakB⁻ cells, PakB-ΔPL recruited dAbp1 to the cell posterior (Figure 4E). We conclude that the interaction with PakB plays a crucial role in dictating the cellular location of dAbp1.

PakB binds actin filaments

The experiments described so far leave unanswered the question as to the mechanism that targets PakB-1-180 to actin-rich regions of the cell. Experiments using a *Dictyostelium* strain that lacks the genes encoding for phosphatidylinositol 3′ kinases (PI3Ks) and PTEN and so cannot produce phosphatidylinositol trisphosphate (PIP_3) showed that PIP_3 was not required to recruit PakB-1-180 to the cell cortex (Supplemental Figure S4; Hoeller and Kay, 2007). Next the requirement for filamentous actin was examined by treating cells with latrunculin A, an inhibitor of actin filament assembly. Latrunculin A caused PakB-GFP to dissociate from the cell cortex and adopt a diffuse cytoplasmic distribution within a few minutes (Figure 5A). This result suggested that the N-terminal region of PakB might interact with actin filaments.

The binding of GST-PakB-1-120 to filamentous actin was examined using an in vitro cosedimentation assay. When centrifuged in the presence of actin filaments GST-PakB-1-120, but not GST (included as an internal control), was depleted from the supernatant (Figure 5B, left). Because GST-PakB-1-120 and actin electrophorese with the same mobility on SDS gels, recovery of GST-PakB-1-120 in the pellet was confirmed by immunoblot analysis using an anti-GST antibody (Figure 5B, right). The immunoblot also showed that a proteolytic fragment of GST-PakB-1-120, ~35 kDa in size, cosedimented with actin (Figure 5B). Based on its size, this fragment likely contains only the N-terminal 60–70 residues of PakB. In agreement with this result, GST-PakB-1-58 was able to bind to actin filaments, albeit more weakly than PakB-1-120 (Figure 5C).

Removal of residues 1–68 from PakB-1-180 resulted in a construct (GFP-PakB-68-180) that had a diffuse cytoplasmic distribution in cells (Figure 5D). PakB-1-58 exhibited a very weak enrichment at the leading edge, whereas PakB-1-79 localized well to the leading edge (Figure 5D). Taken together, the results indicate that an actin-binding module comprising residues ~1–70 is responsible for the localization of PakB to actin-rich regions in the cell.

The failure of dAbp1 to localize to actin-rich sites in the PakB⁻ cells prompted us to examine its ability to bind actin filaments, using a cosedimentation assay. Only a small fraction of GST-dAbp1 was recovered in the actin filament pellet, indicating that the ADF-H domain is not sufficient to mediate a strong interaction between dAbp1 and filamentous actin (Figure 5E). The addition of GST-PakB-1-120

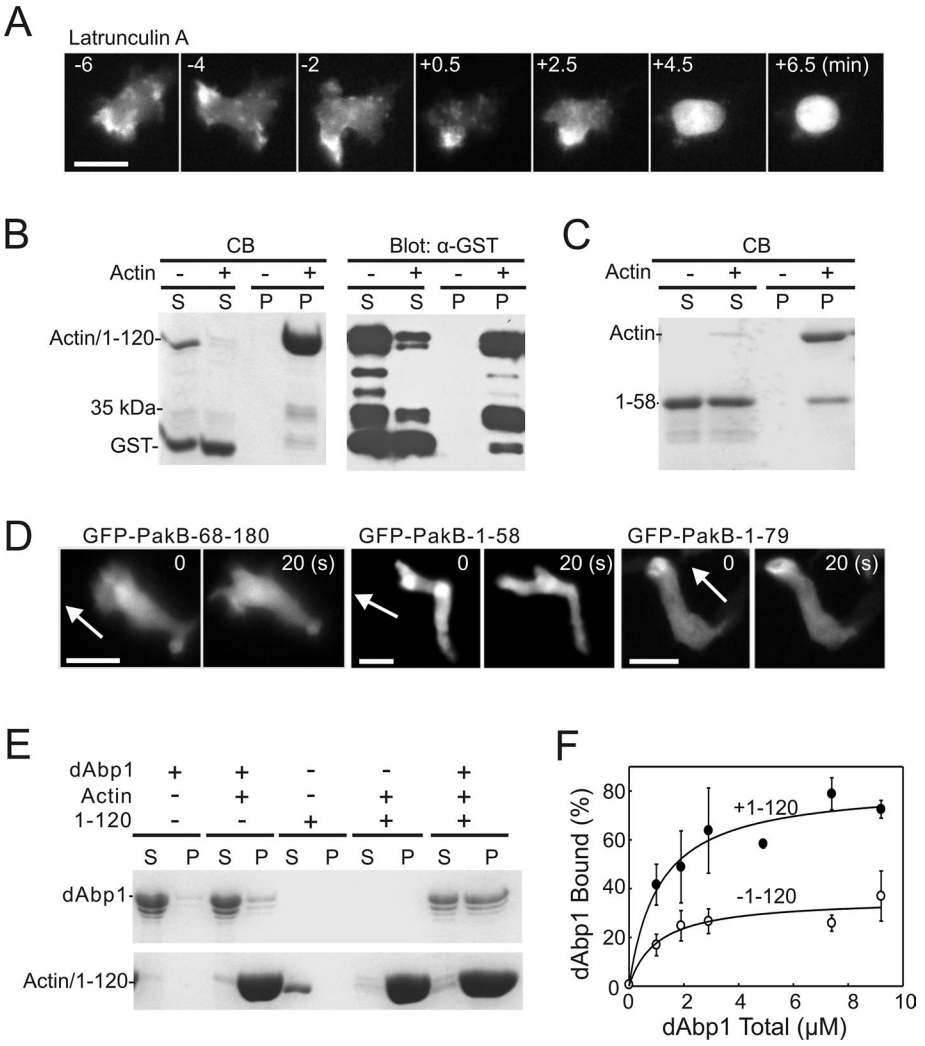

FIGURE 5: The PakB N-terminus binds actin. (A) Time-course images showing the redistribution of PakB-GFP to the cytoplasm after addition of latrunculin A (5 μM) at time 0. Bar, 10 μm. (B, C) Actin filament cosedimentation experiments were performed using (B) GST-PakB-1-120 (1–120) and (C) GST-PakB-1-58 (1–58). Samples were centrifuged at 100,000 × *g* for 30 min, and the resulting supernatants (S) and pellets (P) were subjected to SDS–PAGE and stained with Coomassie blue (B, left; C) or probed with an anti-GST antibody (B, right). Note that GST-PakB-1-120 and actin have the same mobility on SDS–PAGE. (D) Images of developed migrating PakB$^-$ cells expressing GFP-PakB-1-58, GFP-PakB-1-79, or GFP-PakB-68-180. Arrows indicate the direction of migration. Bars, 10 μm. (E) Actin filament cosedimentation experiments were performed with GST-dAbp1 in the presence or absence of GST-PakB-1-120 (1–120). Samples were centrifuged at 100,000 × *g* for 30 min, and the resulting supernatants (S) and pellets (P) were subjected to SDS–PAGE and stained with Coomassie blue. (F) The percentage of GST-dAbp1 that cosedimented with actin in the presence (•) or absence (○) of 5 μM GST-PakB-1-120 was quantified by densitometry of Coomassie blue–stained SDS gels. Results show the mean and SD for three independent experiments.

strongly enhanced the binding of GST-dAbp1 to filamentous actin (Figure 5, E and F). The binding of GST-dAbp1 to actin was too weak to accurately determine a binding constant, but in the presence of an equimolar amount of GST-PakB-1-120 a K_d = 1.1 ± 0.4 μM was obtained. We propose that the actin-associated PakB-1-120 is able to interact with the SH3 domain of dAbp1 and thus serves to enhance the association of dAbp1 to actin filaments.

PakB regulates dAbp1 activity in cells

The overexpression of dAbp1 in *Dictyostelium* has been reported to delay early development, including cell elongation, streaming, and aggregate formation, by several hours (Wang and O'Halloran, 2006). We confirmed this phenotype using the wild-type JH10 cell line. JH10 cells streamed and formed aggregates after 7 h of starvation, whereas JH10 cells expressing RFP-dAbp1 (dAbp1^{OE} cells) took 11 h to elongate and 13–15 h to form streams and aggregates (Figure 6, A and B). We next examined how the expression of RFP-dAbp1 influences early development in PakB$^-$ cells, which stream and form aggregates with a time course equivalent to that of the parental JH10 cells (Figure 6A). Of interest, expression of RFP-dAbp1 completely blocked early development in PakB$^-$ cells (Figure 6B). These cells failed to elongate when placed in starvation buffer and did not stream or form aggregates. After 14 h of starvation, some small clumps of PakB$^-$/dAbp1^{OE} cells were visible, suggesting that they may develop a limited ability to adhere to one other. During chemotaxis in a cAMP gradient PakB$^-$/dAbp1^{OE} cells were unable to maintain a polarized, elongated morphology but underwent rapid and dramatic changes in shape (Figure 6C, Supplemental Figure S3, and Supplemental Video S5). Immunoblot analysis showed that similar levels of RFP-dAbp1 were expressed in JH10 and PakB$^-$ cells (Figure 6D). The amounts of endogenous dAbp1 expressed by PakB$^-$ cells and JH10 cells are also comparable.

We tested whether the block in early development exhibited by PakB$^-$/dAbp1^{OE} cells could be rescued by expression of PakB-1-180. After 14 h in starvation buffer PakB$^-$/dAbp1^{OE} cells expressing GFP-PakB-1-180 formed defined streams and aggregates (Figure 6B). In contrast, the expression of PakB-1-180ΔP, which does not bind the dAbp1 SH3 domain, was unable to reverse the block in early development. At the 14-h time point, 60–80% of PakB$^-$/dAbp1^{OE} cells expressing PakB-1-180 had an elongated morphology, whereas cells expressing PakB-1-180ΔP were rounded or irregularly shaped. Immunoblot analysis showed that equivalent amounts of PakB-1-180 and PakB-1-180ΔP were expressed in PakB$^-$/dAbp1^{OE} cells (Figure 6D).

To test whether the effects of dAbp1 are mediated by its SH3 domain, we expressed a version of dAbp1 with a function-blocking mutation (P474L) in the SH3 domain (dAbp1-ΔSH3) in PakB$^-$ cells. Expression of RFP-dAbp1-ΔSH3 had no effect on the ability of PakB$^-$ cells to complete early development (Figure 6A), even though it was expressed at a level comparable to RFP-dAbp1 (Supplemental Figure S5A). Moreover, RFP-dAbp1-ΔSH3 did not alter the morphology of PakB$^-$ cells during chemotaxis in a cAMP gradient (Supplemental Figure S5A and B). The cells maintained an elongated phenotype during chemotaxis but, as previously reported for PakB$^-$ cells, tended

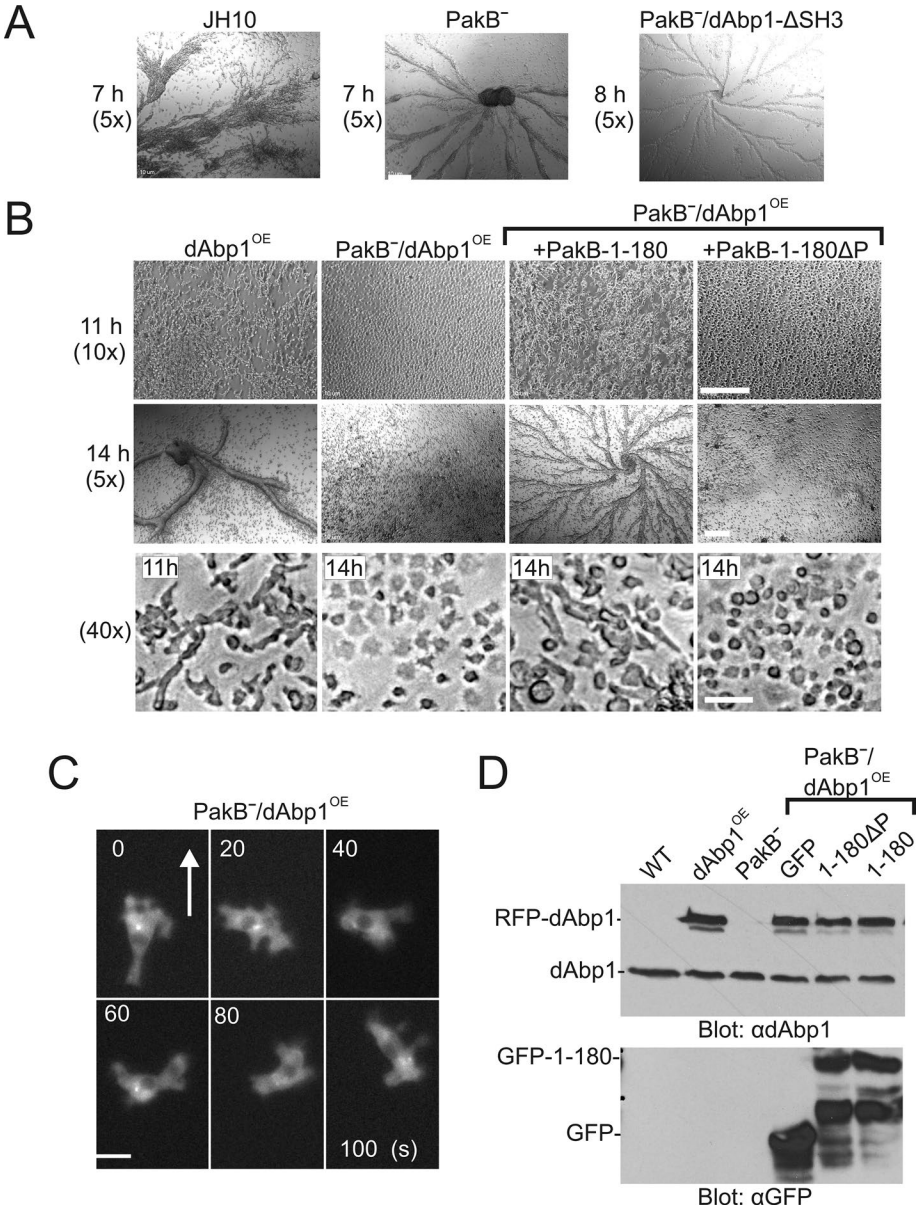

FIGURE 6: Overexpression of dAbp1 blocks development of PakB⁻ cells. (A) JH10 cells, PakB⁻ cells, and PakB⁻ cells expressing RFP-dAbp1 with a function-blocking mutation in its SH3 domain (dAbp1-ΔSH3) were starved to induce development. The cells formed streams and aggregates after 7-8 h of starvation. Magnification, 5×. (B) JH10 cells expressing RFP-dAbp1 (dAbp1^{OE}), PakB⁻ cells expressing RFP-dAbp1 (PakB⁻/dAbp1^{OE}), and PakB⁻/dAbp1^{OE} cells expressing GFP-PakB-1-180 or GFP-PakB-1-180ΔP were starved to induce development and imaged at 7, 11, or 14 h at 5, 10, or 40× magnification as indicated. Bar, 0.2 mm (top, middle), 20 μm (bottom). (C) Time-course images of a developed PakB⁻/dAbp1^{OE} cell migrating in a cAMP gradient. The cell undergoes rapid shape changes, with RFP-dAbp1 diffusely distributed in the cytoplasm. Arrow indicates the direction of migration. Bar, 10 μm. (D) Extracts of the described cell lines were subject to immunoblot analysis using anti-dAbp1 (top) and anti-GFP (bottom) antibodies to show the expression levels of dAbp1, RFP-dAbp1, GFP-PakB-1-180, and PakB-1-180ΔP.

to extend more lateral pseudopods than JH10 cells (Lee *et al.*, 2004).

PakB⁻/ dAbp1^{OE} cells migrate slowly

The chemotactic properties of JH10, dAbp1^{OE}, PakB⁻, and PakB⁻/ dAbp1^{OE} cells in a stable cAMP gradient were examined in more detail using Ibidi μ-slides. dAbp1^{OE} cells moved ~30% faster than JH10 cells, with no significant loss in directionality (calculated by dividing the Euclidean distance traveled in the direction of the cAMP gradient by the total accumulated distance) (Figure 7, A and B). PakB⁻ cells migrated ~30% more slowly than the parental JH10 cells and made sharp, rapid turns, resulting in a decreased directionality. PakB⁻/dAbp1^{OE} cells exhibited a directionality similar to that of PakB⁻ cells, showing that they can sense and respond to the cAMP gradient. However, their speed was ~30% less than that of PakB⁻ cells, which likely reflects the fact that they cannot maintain a polarized morphology. The speed of the PakB⁻/dAbp1^{OE} cells was increased nearly to the level of PakB⁻ cells by the expression of GFP-PakB-1-180 but was not significantly altered by expression of GFP or GFP-PakB-1-180ΔP. Taken together, the results show that PakB plays an important role in controlling the cellular activities of dAbp1.

DISCUSSION

PakB localizes to actin-rich membrane protrusions, where it is implicated in the phosphorylation and activation of class I myosins (De La Roche *et al.*, 2005). Here we show that the N-terminal regulatory region of PakB contains an actin filament–binding module and two docking sites for the SH3 domain of dAbp1. PakB localizes dAbp1 to actin-rich sites at the plasma membrane and plays a critical role in regulating its cellular activities. In turn, dAbp1 may facilitate the recruitment of class I myosins to PakB in order to promote their activation.

Tandem proline-rich motifs bind the dAbp1 SH3 domain

Two closely spaced binding sites for the SH3 domain of dAbp1 were identified in the N-terminal region of PakB. The two sites (P2 and P3/4) share a PxxPx$_{(0-2)}$RP motif (Figure 8A). Mutation of the first proline residue in the motif blocks the binding of the dAbp1 SH3 domain, but other key recognition determinants for the dAbp1 SH3 domain remain to be identified. Disruption of both the P2 and P3/4 motifs is needed to abolish binding of the dAbp1 SH3 domain to PakB, indicating that each site can individually bind the SH3 domain. Nevertheless, the two PxxPx$_{(0-2)}$RP motifs are separated by only 11 residues and so could function in a cooperative or mutually exclusive manner. In this context it is interesting to note that the SH3 domain of yeast Abp1 SH3 domain binds to an extended target sequence 17 residues in length (Fazi *et al.*, 2002; Stollar *et al.*, 2009). If the target sequence recognized by the dAbp1 SH3 domain is of similar length, then simultaneous binding of the dAbp1 SH3 domain to the P2 and P3/4 may not be possible. Further studies to

A

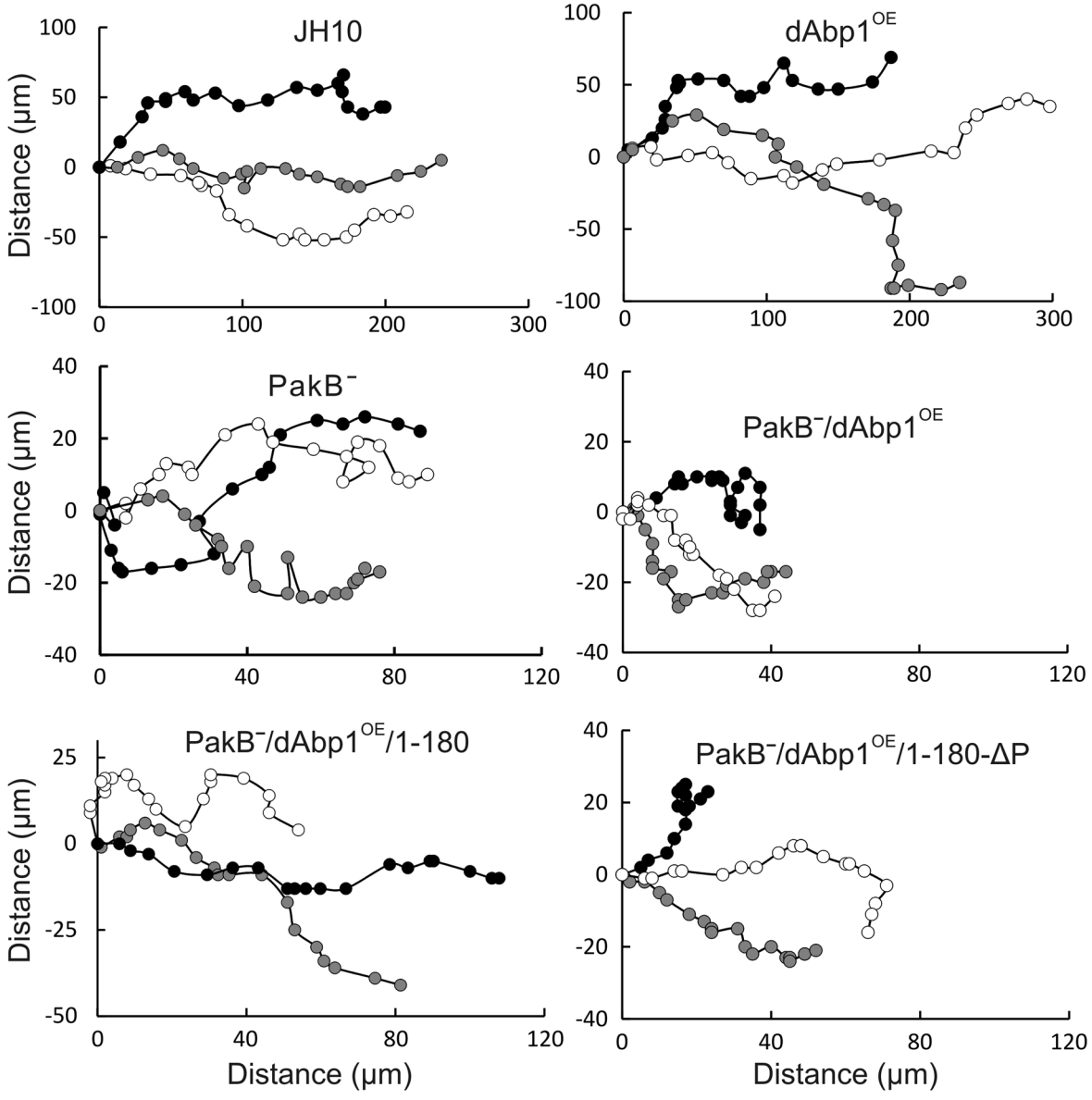

B

	JH10	dAbp1^{OE}	PakB^{-}	PakB^{-}/dAbp1^{OE} None	PakB^{-}/dAbp1^{OE} +GFP	PakB^{-}/dAbp1^{OE} +1-180	PakB^{-}/dAbp1^{OE} +1-180ΔP
Speed (μm/min)	15.0 ± 7.1	19.5 ± 8.3	10.5 ± 2.8	7.0 ± 2.2	7.4 ± 2.4	9.8 ± 2.0	7.3 ± 2.3
	P<0.01	P<1E-8	P<1E-9	P<1E-8			
Directionality	0.61 ± 0.24	0.58 ± 0.31	0.49 ± 0.16	0.48 ± 0.19	0.41 ± 0.18	0.48 ± 0.20	0.60 ± 0.22
	P<0.0001						

FIGURE 7: Overexpression of dAbp1 in PakB^{-} cells inhibits chemotaxis. (A) Developed cells were monitored during chemotaxis in a linear and stable cAMP gradient using Ibidi μ-slides. Positions were recorded every 30 s. Typical tracks for three cells from each of the indicated cell lines are shown. (B) Speed and directionality values were calculated for each cell line using the Ibidi Chemotaxis and Migration Tool 2.0. Results show the mean and standard deviations for 15–20 cells in each of three separate experiments. Cells were tracked for a total of 20 min.

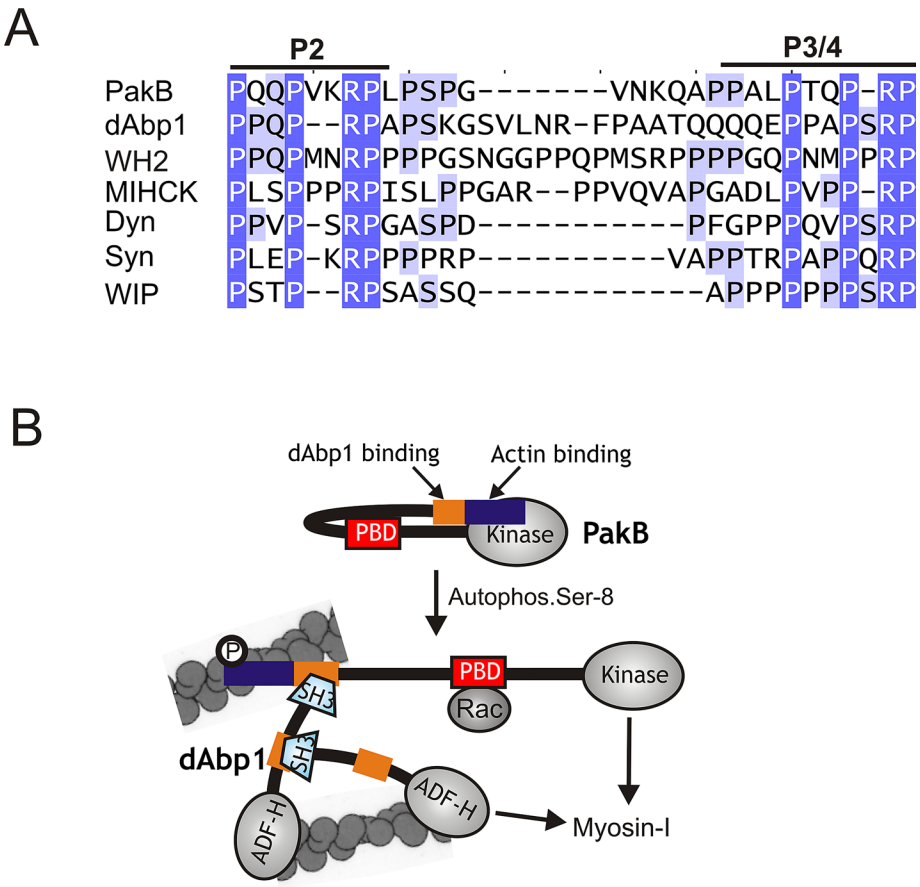

FIGURE 8: PakB interacts with the dAbp1 SH3 domain via a conserved proline-rich sequence. (A) Sequences similar to the two binding sites for the dAbp1 SH3 domain in PakB (P2 and P3/4; residues 64–91) are conserved in dAbp1 (residues 265–297), a *Dictyostelium* WH2 domain–containing protein (WH2; residues 361-396), *Acanthamoeba* myosin I heavy chain kinase (MIHCK; residues 207–239), human dynamin-1 (Dyn; residues 813–836); human synaptojanin-1 (Syn; residues 1141–1165), and human WAS/WASL-interacting protein family member 1 (WIP-1; residues 295–316). GenBank accession numbers are as follows: WH2 domain-containing protein (EAL66623), MIHCK (AAD09141), dynamin-1 (AAH50279), synaptojanin-1 (NP_003886), and WIP-1 (NP_003378). (B) A model for the PakB–dAbp1 complex. Inactive PakB is believed to adopt a folded conformation in which the N-terminal region suppresses the activity of the PBD and kinase domains. Autophosphorylation of Ser-8, which occurs in the absence of allosteric effectors, allows GTP-Rac to bind the PBD domain (red box) and increases kinase activity 40-fold. It is proposed that Ser-8 autophosphorylation causes PakB to unfold, which would increase exposure of the N-terminal region that contains an actin-binding module (blue box) and binding sites for the dAbp1 SH3 domain (orange box). The actin-binding module recruits PakB to actin-rich regions at the cell cortex, where it serves as a docking site for dAbp1. Whether the P2 and P3/4 motifs can support the concurrent binding of two dAbp1 molecules is not known. dAbp1 contains an ADF-H domain that weakly binds actin filaments and a P2-P3/4-like sequence (orange) that binds its own SH3 domain, suggesting that dimers or oligomers of dAbp1 may assemble to cross-link and strengthen the local actin network. dAbp1 interacts directly with MyoK, and possibly other class I myosins, suggesting that it may facilitate their recruitment to the complex to be phosphorylated and activated by PakB.

determine whether the stoichiometry of the PakB-dAbp1 complex is 1:1 or 1:2 should resolve this question.

Tandem PxxPx$_{(0-2)}$RP motifs occur within the GPA domain of dAbp1 (Figures 2A and 8A). Pull-down assays confirmed that this region of dAbp1 is capable of binding to the dAbp1 SH3 domain. The presence of an internal binding site for its SH3 domain raises the possibility that dAbp1 can adopt a folded conformation or, alternatively, assemble via intermolecular interactions to form dimers or higher-order oligomers (Figure 8B). In the latter case, a PakB–dAbp1 complex would encompass multiple actin-binding modules and could function to cross-link and organize actin filaments within membrane protrusions.

The results suggest that tandem PxxPx$_{(0-2)}$RP motifs may function as specific binding sites for the dAbp1 SH3 domain. Pattern Hit Initiated BLAST searches identified multiple examples of this motif in an uncharacterized *Dictyostelium* protein with a Wiskott–Aldrich syndrome homology region 2 (WH2) domain (dictyBase DDB_G0281723; Figure 8A). Tandem PxxPx$_{(0-2)}$RP motifs are also present in the N-terminal region of *Acanthamoeba* myosin I heavy chain kinase (MIHCK), a PAK-family kinase that phosphorylates and activates class I myosins (Brzeska *et al.*, 1999). The presence of these motifs suggests that recruitment of Abp1 by MIHCK may be involved in the regulation of myosin I activity in *Acanthamoeba*. Several proteins known to bind the SH3 domain of mammalian Abp1 (mAbp1), including dynamin, synaptojanin-1, and WASp-interacting protein family member 1, contain tandem PxxPx$_{(0-2)}$RP motifs (Figure 8A; Kessels *et al.*, 2001; Cortesio *et al.*, 2010). Whether these sequences function as specific binding sites for the SH3 domain of mammalian Abp1 requires further study.

Regulatory functions of the N-terminal region of PakB

The first ~70 residues of PakB bind to actin filaments and target PakB to actin-rich regions at the cell cortex. The discovery of the actin filament–binding module provides an explanation for the behavior of PakB-1-276, PakB-ΔC, and PakB-ΔPL, which aggregate into dot-like particles that mislocalize to the rear of migrating cells (Figure 1D; De La Roche *et al.*, 2005). We propose that the 180–276 sequence, which is hydrophobic and contains few charged residues, causes these constructs to aggregate. Because the aggregates contain multiple actin-binding modules, they bind very tightly to actin filaments. The dot-like particles formed by PakB-1-276, PakB-ΔC, and PakB-ΔPL exhibit a cellular distribution very similar to that of injected phalloidin and other constructs that bind with high affinity to actin filaments (De La Roche *et al.*, 2005).

Database searches did not detect sequences similar to PakB-1-70 in other proteins, but it is possible that only a small subset of residues within this sequence makes critical contacts with the actin filament. It is intriguing that myosin heavy chain kinase-A (MHCK-A), which inhibits myosin II filament assembly, is targeted to the same cellular sites as PakB, including the leading edge of cells and phagocytic cups, by an N-terminal actin filament-binding module (Steimle *et al.*, 2002; Russ *et al.*, 2006). The respective actin-binding modules may allow PakB and MHCK-A to coordinate activation of myosin I and inhibition of myosin II at actin-rich sites.

The N-terminus of PakB has been described as a negative regulatory element that suppresses the activity of the PBD and kinase domains (Figure 8B; Lee *et al.*, 1996, 1998; Lee and Côté, 1995). The first step in the activation of PakB is the autophosphorylation of Ser-8. This reaction is believed to relieve the inhibitory effects of the N-terminal region by converting PakB from a closed, inactive state to an open, active state (Figure 8B; Lee *et al.*, 1998). The results of this study show that Ser-8 is located within the actin-binding module of PakB. Studies are underway to investigate the effect of Ser-8 autophosphorylation on the ability of PakB to bind to actin filaments.

PakB promotes binding of dAbp1 to actin filaments

Actin filament cosedimentation assays showed that dAbp1 has a low affinity for actin filaments. In contrast, mAbp1 and drebrin, a homologue of mAbp1, bind tightly to actin (Kessels *et al.*, 2000; Grintsevich *et al.*, 2010). Both mAbp1 and drebrin contain two distinct actin-binding modules: the ADF-H domain and a charged α-helical sequence. In the absence of the charged α-helical sequence the ADF-H domains of mAbp1 and drebrin bind weakly or not at all to filamentous actin (Kessels *et al.*, 2000; Grintsevich *et al.*, 2010). Sequence alignments show that dAbp1 lacks the charged α-helical sequence present in mAbp1 and drebrin and thus can attach to actin filaments only via its ADF-H domain. PakB enhances the binding of dAbp1 to actin filaments in vitro and is needed to recruit dAbp1 to actin-rich sites in cells. It can be proposed that PakB compensates for the lack of a second intrinsic actin-binding module by providing a means for dAbp1 to attach to actin filaments via its SH3 domain (Figure 8B). The presence of actin-binding modules in both PakB and dAbp1 suggests that the PakB–dAbp1 complex could play an important role in cross-linking and organizing actin filaments (Figure 8B).

dAbp1 interacts with class I myosins

There is emerging evidence that dAbp1 interacts with class I myosins. dAbp1 binds directly to the TH2-like insert in the motor domain of MyoK (Dieckmann *et al.*, 2010) and is recruited to late phagosomes by MyoB (Gopaldass *et al.*, 2012). Studies on the SH3 domain of yeast Abp1 identified the class I myosin Myo5p as a binding partner (Fazi *et al.*, 2002). Given these results, it can be proposed that dAbp1 may function to recruit class I myosins to the PakB–dAbp1 complex in order to facilitate their phosphorylation and activation by PakB. In this model, either the loss or the overexpression of dAbp1 could disrupt formation of a PakB-dAbp1-myosin I complex and result in decreased myosin I motor activity. This model is consistent with the finding that cells that lack or overexpress dAbp1 are unable to suppress the extension of lateral pseudopods during chemotaxis (Wang and O'Halloran, 2006), a defect characteristic of cells that lack one or more class I myosins (Titus *et al.*, 1993; Wessels *et al.*, 1996; Falk *et al.*, 2003).

PakB regulates the cellular functions of dAbp1

The overexpression of dAbp1 had a much more severe effect on the morphology and early development of PakB$^-$ cells than wild-type cells. This result can be considered an example of synthetic dosage lethality (SDL), in which increased amounts of a protein do not produce a noticeable phenotype in a wild-type strain but cause a clear phenotype, such as slow growth or lethality, in a mutant strain with reduced levels of an interacting protein (Prelich, 2012). Of note, genome-wide SDL screens were successful in identifying downstream targets of the Pho85 cyclin-dependent kinase (Sopko *et al.*, 2006). Our overexpression data support the view that the interaction with PakB regulates dAbp1 activity in cells; however, further studies are needed to demonstrate that under normal cellular conditions the activity of dAbp1 is regulated by PakB.

Because overexpression phenotypes often result from competition-based mechanisms, they can also be reversed by co-overexpression of a target protein. We found that the inhibitory effects of dAbp1 on PakB$^-$ cells could be rescued by expression of PakB-1-180, which binds the dAbp1 SH3 domain, and could be abrogated by the introduction of a function-blocking mutation into the dAbp1 SH3 domain. The results show that the effects of dAbp1 on PakB$^-$ cells are mediated by its SH3 domain. This conclusion is consistent with a study showing that the defects resulting from the overexpression of dAbp1, which include a delay in early development and the extension of multiple pseudopods during chemotaxis, are mimicked by overexpression of the SH3 domain (Wang and O'Halloran, 2006). One important function of PakB may therefore be to bind and sequester the dAbp1 SH3 domain, thus limiting its ability to interact with other binding partners.

There is evidence that dAbp1 binds MyoB, MyoK, dynamin A, and profilin II, but whether these interactions are mediated by the dAbp1 SH3 domain or can account for the effects of dAbp1 on cell function remain to be determined (Dieckmann *et al.*, 2010). The studies reported here, which identify a consensus binding sequence for the dAbp1 SH3 domain, should aid in the search for novel binding partners. As noted, one possible candidate is a WH2 domain–containing protein that contains multiple tandem $PxxPx_{(0-2)}RP$ motifs.

In summary, the studies reported here show that dAbp1 binds to PakB via its SH3 domain. The PakB–dAbp1 complex may facilitate the phosphorylation and activation of class I myosins and participate in the cross-linking of actin filaments within membrane protrusions. In addition, the interaction with PakB localizes dAbp1 to actin-rich sites at the plasma membrane and is likely to play a key role in controlling and limiting the ability of the dAbp1 SH3 domain to influence other critical cell signaling pathways.

MATERIALS AND METHODS

Cell growth and development

Dictyostelium AX3 and JH10 strains were grown in tissue culture plates in HL5 medium supplemented with 100 U/ml penicillin and 10 µg/ml streptomycin (Sussman, 1987). PakB$^-$ cells generated in the JH10 background have been described previously (De La Roche *et al.*, 2005). dAbp1-null cells, generated in the AX2 background, were a gift from T. Soldati (University of Geneva, Geneva, Switzerland) and were maintained in HL5 supplemented with 5 µg/ml blasticidin (Life Technologies, Carlsbad, CA; Dieckmann *et al.*, 2010). A pikA-/pikB-/pikC-/pikF-/pikG-/pten- strain that cannot produce PIP_3 was obtained for dictyBase (strain ID DBS0252654; Hoeller and Kay, 2007). Cells expressing GFP or RFP fusion protein constructs were selected and maintained in HL5 supplemented with 5 µg/ml blasticidin or 10 µg/ml G418 (Life Technologies). Development was initiated by taking cells in the log phase of growth and suspending them in development buffer (DB; 5 mM KH_2PO_4, 5 mM Na_2HPO_4, 1 mM $CaCl_2$, 2 mM $MgCl_2$, pH 6.5) at a final density of 10^7 cells/ml. Cells were placed into six-well cell culture plates, and early development was imaged using a Zeiss Axiovert 100 inverted microscope equipped with Plan-Neofluar 5×/0.15, 10×/0.3, and 20×/0.5 objectives (Carl Zeiss, Jena, Germany). To obtain sufficient cells for immunoblot analysis, development was also carried out on Whatman #50 filters (Whatman, Piscataway, NJ; Fey *et al.*, 2007).

DNA constructs and recombinant protein expression

The dAbp1 coding sequence was obtained by reverse transcription-PCR using total RNA as the template, and then amplified using the Expand High Fidelity PCR System (Roche Diagnostics, Indianapolis, IN) and cloned using the TOPO TA Cloning Kit (Life Technologies; De La Roche *et al*., 2005). An N-terminal RFP-dAbp1 fusion protein construct was generated by cloning dAbp1 DNA into the pDbsrXP-mRFP expression vector (Dubin and Nellen, 2010). The N-terminal GFP-PakB fusion protein constructs were generated by cloning PakB DNA, generated by PCR, into the pDXA-GFP2 expression vector (Levi *et al.*, 2000). The N-terminal GST fusion proteins and His-tagged proteins were generated by cloning DNA encoding dAbp1, dAbp1-237-313, and the SH3 domains of dAbp1 (residues 426–481), MyoB (residues 1058–1105), and MyoC (residues 1128–1176) into pGEX-4T (GE Healthcare, Piscataway, NJ) or pET28a (Novagen, Gibbstown, NJ) plasmids. Site-directed mutagenesis was carried out using the Stratagene QuikChange Site-Directed Mutagenesis Kit (Agilent Technologies, Santa Clara, CA). *Dictyostelium* cells were transformed by electroporation as described (De La Roche *et al*., 2005). Bacterial protein expression used BL21(DE3) cells. Cells grown to an $OD_{600\ nm}$ of 0.6–0.8 were induced by the addition of isopropyl β-D-1-thiogalactopyranoside to a final concentration of 0.2 mM. GST fusion proteins were purified using glutathione-Sepharose 4B beads (GE Healthcare), and His-tagged proteins were purified using His-Bind Resin (Novagen).

Yeast two-hybrid analysis

A bait plasmid was constructed by inserting a DNA fragment encoding amino acids 1–187 of PakB in-frame with the Lex202 DNA–binding domain in the vector pEG202 (Gyuris *et al*., 1993). The bait plasmid was transformed into the *Saccharomyces cerevisiae* reporter strain W303. Two-hybrid experiments were performed by transforming the W303-bait strain with a pACT2 yeast two-hybrid cDNA library generated from size-selected (0.5–5 kb) RNA isolated from growth-phase *Dictyostelium* (kindly provided by A. Kuspa, Baylor College of Medicine, Houston, TX). Interaction analysis was performed by growing transformants on selective minimal medium lacking leucine, histidine, and adenine. Positive clones were re-screened for the activation of the β-galactosidase reporter by liquid culture assay using standard protocols. Library plasmids were extracted from positive yeast clones, separated from bait plasmids by transformation of DH5α cells, and reintroduced into the W303 yeast strain together with the original bait plasmid or the control pEG202 plasmid to confirm interactions. Inserts of plasmids that overcame these selective steps were sequenced. Additional interaction assays were performed by cloning DNA encoding the dAbp1 SH3 domain into pACT2 (Clontech, Mountain View, CA).

Coimmunoprecipitation assays and Western blots

Dictyostelium cells were mechanically lysed using a 5-μm–pore size Nuclepore membrane (Whatman). Cells in lysis buffer (0.5× phosphate-buffered saline (PBS), 1 mM EDTA, 0.2% NP-40, 10% glycerol) supplemented with 1× Protease Inhibitor Cocktail (Sigma-Aldrich, St. Louis, MO) were passed twice through the membrane and then were centrifuged at 15,000 × *g* for 30 min. The resulting supernatants were incubated for 1 h on ice with an affinity-purified rabbit polyclonal antibody raised against GST-dAbp1, a rabbit polyclonal anti-PakB antibody (De La Roche *et al*., 2005), or monoclonal and polyclonal anti-GFP antibodies (sc-9996, Santa Cruz Biotechnology, Santa Cruz, CA; and AB3080P, EMD Millipore, Billerica, MA). Immune complexes were isolated by addition of 25 μl of protein A–Sepharose beads (Sigma-Aldrich) and washed five times with lysis buffer. Pull-down assays were performed by adding 20 μl of glutathione–Sepharose 4B beads and 20 μg of purified GST-SH3 domain to 1 ml of the supernatant fraction prepared from 4×10^7 cells. After 1 h on ice the beads were collected by centrifugation and washed three times with lysis buffer. Samples were then boiled in 50 μl of 2× SDS sample buffer, subjected to SDS–PAGE, and transferred to Immobilon-P membranes (Millipore) for Western blot analysis using the antibodies described or an anti-GST antibody (27-4577-01; GE Healthcare). Blots were incubated with goat anti-rabbit and goat anti-mouse second antibodies coupled to horseradish peroxidase (Bio-Rad Laboratories, Hercules, CA) and visualized using Western Lightning Plus reagent (PerkinElmer, Waltham, MA).

Actin cosedimentation assay

Actin binding assays were performed using the Actin Binding Protein Spin Down Biochem Kit (Cytoskeleton, Denver, CO) according to the manufacturer's instructions. GST-PakB and dAbp1 proteins (2–4 μM) were incubated at room temperature for 10 min with or without 8.5 μM rabbit muscle actin in 50 mM KCl, 10 μM $CaCl_2$, 2 mM $MgCl_2$, 1 mM ATP, 65 mM Tris-HCl, pH 6.5, and 1× Protease Inhibitor Cocktail. Experiments to measure the binding of GST-dAbp1 to actin contained 0.2 μM GST-dAbp1, 0 or 0.2 μM GST-PakB-1-120, and 0.2 μM GST. Samples were centrifuged in a Beckman TLA 100 rotor at 100,000 × *g* for 30 min. The supernatants were removed and the pellets carefully washed in binding buffer and resuspended to the original volume in SDS gel sample buffer. Equal volumes of the supernatants and pellets were resolved by SDS–PAGE. Gels were stained with Coomassie blue or processed for Western blot analysis using an anti-GST antibody and then scanned using a densitometer to determine the amount of GST-dAbp1 in the pellet.

Cell imaging and chemotaxis assays

Immunofluorescence images were obtained for cells attached to glass coverslips after washing in 15 mM Na/KPO_4 buffer, pH 6.5, fixation in ice-cold 95% methanol, and permeabilization with 70% ethanol. After blocking with 20% normal goat serum (NGS; Invitrogen, Carlsbad, CA), cells were incubated with primary antibodies in 20% NGS, washed extensively with PBS, and incubated with goat anti-rabbit and anti-mouse antibodies coupled to Alexa Fluor 488 or Alexa Fluor 633 (Life Technologies). To obtain aggregation competent cells for use in chemotaxis experiments, cells were shaken in DB at 150 rpm and pulsed with cAMP (final concentration, 200 nM) every 6 min for 4–7 h (Gerisch, 2009). Aggregation-competent cells were placed onto a coverslip and directionally stimulated using a Femtotip (Eppendorf, Hauppauge, NY) filled with 10 μM cAMP (Gerisch, 2009). Fluorescence images were obtained using a Zeiss Axiovert 100 inverted microscope equipped with a Plan-Neofluar 40×/0.75 objective. Chemotaxis in a stable cAMP gradient was examined by loading a 6-μl aliquot of aggregation-competent cells (3×10^6 cells/ml) onto Chemotaxis 3D μ-slides (Ibidi, Munich, Germany). After 30 min, one reservoir on the slide was filled with DB and the other with DB containing 100 nM cAMP. Fluorescence images were captured using a Zeiss Axiovert 100 inverted microscope equipped with a Plan-Neofluar 10×/0.3 objective. Migration tracks for 30–45 cells for each cell line were collected from at least three different μ-slides. Speed and directionality were calculated over a 20-min period using Ibidi Chemotaxis and Migration Tool 2.0. Directionality, a measure of the linearity of the pathway, was calculated by dividing the Euclidean distance traveled in the direction of the cAMP gradient by the accumulated distance traveled.

ACKNOWLEDGMENTS

This research was funded by a Natural Sciences and Engineering Research Council of Canada Discovery Grant and a Canadian Institutes of Health Research Operating Grant (MOP8603) to G.P.C. We thank Adam Kuspa for providing the yeast two-hybrid cDNA library, Charlie Boone (University of Toronto) for help with the yeast two-hybrid screens, and Thierry Soldati for providing the dAbp1-null cell line. Fluorescence microscopy was carried out at the Queen's University Protein Function Discovery Facility (Kingston, Canada).

REFERENCES

Bement WM, Mooseker MS (1995). TEDS rule: a molecular rationale for differential regulation of myosins by phosphorylation of the heavy chain head. Cell Motil Cytoskeleton 31, 87–92.

Brzeska H, Young R, Knaus U, Korn ED (1999). Myosin I heavy chain kinase: cloning of the full-length gene and acidic lipid-dependent activation by rac and cdc42. Proc Natl Acad Sci USA 96, 394–399.

Chen CL, Wang Y, Sesaki H, Iijima M (2012). Myosin I links PIP3 signaling to remodeling of the actin cytoskeleton in chemotaxis. Sci Signal 5, ra10.

Cortesio CL, Perrin BJ, Bennin DA, Huttenlocher A (2010). Actin-binding protein-1 interacts with WASp-interacting protein to regulate growth factor-induced dorsal ruffle formation. Mol Biol Cell 21, 186–197.

Dai J, Ting-Beall HP, Hochmuth RM, Sheetz MP, Titus MA (1999). Myosin I contributes to the generation of resting cortical tension. Biophys J 77, 1168–1176.

De La Roche MA, Mahasneh A, Lee S-F, Rivero F, Côté GP (2005). Cellular distribution and functions of wild-type and constitutively activated *Dictyostelium* PakB. Mol Biol Cell 16, 238–247.

Dieckmann R *et al*. (2010). A myosin IK-Abp1-PakB circuit acts as a switch to regulate phagocytosis efficiency. Mol Biol Cell 21, 1505–1518.

Dubin M, Nellen W (2010). A versatile set of tagged expression vectors to monitor protein localisation and function in *Dictyostelium*. Gene 465, 1–8.

Durrwang U, Fujita-Becker S, Erent M, Kull FJ, Tsiavaliaris G, Geeves MA, Manstein DJ (2006). *Dictyostelium* myosin-IE is a fast molecular motor involved in phagocytosis. J Cell Sci 119, 550–558.

Falk DL, Wessels D, Jenkins L, Pham T, Kuhl S, Titus MA, Soll DR (2003). Shared, unique and redundant functions of three members of the class I myosins (MyoA, MyoB and MyoF) in motility and chemotaxis in *Dictyostelium*. J Cell Sci 116, 3985–3999.

Fazi B, Cope MJ, Douangamath A, Ferracuti S, Schirwitz K, Zucconi A, Drubin DG, Wilmanns M, Cesareni G, Castagnoli L (2002). Unusual binding properties of the SH3 domain of the yeast actin-binding protein Abp1: structural and functional analysis. J Biol Chem 277, 5290–5298.

Fey P, Kowal AS, Gaudet P, Pilcher KE, Chisholm RL (2007). Protocols for growth and development of *Dictyostelium discoideum*. Nat Protoc 2, 1307–1316.

Fujita-Becker S, Durrwang U, Erent M, Clark RJ, Geeves MA, Manstein DJ (2004). Changes in Mg2+-Ion concentration and heavy chain phosphorylation regulate the motor activity of a class-I myosin. J Biol Chem 280, 6064–6071.

Gerisch G (2009). Imaging actin cytoskeleton dynamics in *Dictyostelium* chemotaxis. Methods Mol Biol 571, 385–400.

Gopaldass N *et al*. (2012). Dynamin A, myosin IB and Abp1 couple phagosome maturation to F-actin binding. Traffic 13, 120–130.

Grintsevich EE, Galkin VE, Orlova A, Ytterberg AJ, Mikati MM, Kudryashov DS, Loo JA, Egelman EH, Reisler E (2010). Mapping of drebrin binding site on F-actin. J Mol Biol 398, 542–554.

Gyuris J, Golemis E, Chertkov H, Brent R (1993). Cdi1, a human G1 and S phase protein phosphatase that associates with Cdk2. Cell 75, 791–803.

Hoeller O, Kay RR (2007). Chemotaxis in the absence of PIP3 gradients. Curr Biol 17, 813–817.

Jung G, Remmert K, Wu X, Volosky JM, Hammer JA III (2001). The *Dictyostelium* CARMIL protein links capping protein and the Arp2/3 complex to Type I myosins through their SH3 domains. J Cell Biol 153, 1479–1498.

Jung G, Wu XF, Hammer JA III (1996). *Dictyostelium* mutants lacking multiple classic myosin I isoforms reveal combinations of shared and distinct functions. J Cell Biol 133, 305–323.

Kessels MM, Engqvist-Goldstein AE, Drubin DG (2000). Association of mouse actin-binding protein 1 (mAbp1/SH3P7), an src kinase target, with dynamic regions of the cortical actin cytoskeleton in response to rac1 activation. Mol Biol Cell 11, 393–412.

Kessels MM, Engqvist-Goldstein AE, Drubin DG, Qualmann B (2001). Mammalian Abp1, a signal-responsive F-actin-binding protein, links the actin cytoskeleton to endocytosis via the GTPase dynamin. J Cell Biol 153, 351–366.

Lee S-F, Côté GP (1995). Purification and characterization of a *Dictyostelium* protein kinase required for the actin-activated MgATPase activity of *Dictyostelium* myosin ID. J Biol Chem 270, 11776–11782.

Lee S-F, Egelhoff TT, Mahasneh A, Côté GP (1996). Cloning and characterization of a *Dictyostelium* myosin I heavy chain kinase activated by Cdc42 and Rac. J Biol Chem 271, 27044–27048.

Lee S-F, Mahasneh A, De La Roche MA, Côté GP (1998). Regulation of the PAK-related *Dictyostelium* myosin I heavy chain kinase by autophosphorylation, acidic phospholipids and Ca^{2+}-calmodulin. J Biol Chem 273, 27911–27917.

Lee S, Rivero F, Park KC, Huang E, Funamoto S, Firtel RA (2004). *Dictyostelium* PAKc Is required for proper chemotaxis. Mol Biol Cell 15, 5456–5469.

Levi S, Polyakov M, Egelhoff TT (2000). Green fluorescent protein and epitope tag fusion vectors for *Dictyostelium discoideum*. Plasmid 44, 231–238.

McConnell RE, Tyska MJ (2010). Leveraging the membrane—cytoskeleton interface with myosin-1. Trends Cell Biol 20, 418–426.

Novak KD, Peterson MD, Reedy MC, Titus MA (1995). *Dictyostelium* myosin I double mutants exhibit conditional defects in pinocytosis. J Cell Biol 131, 1205–1221.

Novak KD, Titus MA (1998). The myosin I SH3 domain and TEDS rule phosphorylation site are required for in vivo function. Mol Biol Cell 9, 75–88.

Pang KM, Lee E, Knecht DA (1998). Use of a fusion protein between GFP and an actin-binding domain to visualize transient filamentous-actin structures. Curr Biol 8, 405–408.

Prelich G (2012). Gene overexpression: uses, mechanisms, and interpretation. Genetics 190, 841–854.

Russ M, Croft D, Ali O, Martinez R, Steimle PA (2006). Myosin heavy-chain kinase A from *Dictyostelium* possesses a novel actin-binding domain that cross-links actin filaments. Biochem J 395, 373–383.

Schwarz EC, Neuhaus EM, Kistler C, Henkel AW, Soldati T (2000). *Dictyostelium* myosin IK is involved in the maintenance of cortical tension and affects motility and phagocytosis. J Cell Sci 113, 621–633.

Sopko R *et al*. (2006). Mapping pathways and phenotypes by systematic gene overexpression. Mol Cell 21, 319–330.

Steimle PA, Licate L, Côté GP, Egelhoff TT (2002). Lamellipodial localization of *Dictyostelium* myosin heavy chain kinase A is mediated via F-actin binding by the coiled-coil domain. FEBS Lett 516, 58–62.

Stollar EJ, Garcia B, Chong PA, Rath A, Lin H, Forman-Kay JD, Davidson AR (2009). Structural, functional, and bioinformatic studies demonstrate the crucial role of an extended peptide binding site for the SH3 domain of yeast Abp1p. J Biol Chem 284, 26918–26927.

Sussman M (1987). Cultivation and synchronous morphogenesis of *Dictyostelium* under controlled experimental conditions. Methods Cell Biol 28, 9–29.

Titus MA, Wessels D, Spudich JA, Soll D (1993). The unconventional myosin encoded by the *myo*A gene plays a role in *Dictyostelium* motility. Mol Biol Cell 4, 233–246.

Wang Y, O'Halloran TJ (2006). Abp1 regulates pseudopodium number in chemotaxing *Dictyostelium* cells. J Cell Sci 119, 702–710.

Wessels D, Titus MA, Soll DR (1996). A *Dictyostelium* myosin I plays a crucial role in regulating the frequency of pseudopods formed on the substratum. Cell Motil Cytoskeleton 33, 64–79.